Local electronic structure investigation of the sol-gel processed calcium hydroxide material

Jitendra Pal Singh*, So Hee Kim, Weon Cheol Lim, Sung Ok Won, Keun Hwa Chae*

Advanced Analysis Center, Korea Institute of Science and Technology, Seoul 02792, Korea

*Corresponding author

DOI: 10.5185/amp.2018/887
www.vbripress.com/amp

Abstract

In the present work, we have reported the synthesis of calcium hydroxide from calcium nitrate. Synthesized nanoparticles were characterized using X-ray diffraction, scanning electron micrographs, and near edge X-ray absorption fine structure measurements. Synthesized nanoparticles exhibit tetragonal phase with space group P3m1. These nanoparticles exhibit almost spherical shape. Particle size of these nanoparticles are 55 nm and 69 nm for two different treatment of precursor. Microscopic studies shows that size distribution is affected by the change of thermal history. Local electronic structure measured at Ca (*L*- & *K*-) and O *K*-edges exhibit presence of spectral features that are characteristics of calcium hydroxide. Moreover, strength and magnitude of crystal field parameter is unaffected by thermal treatment utilized for synthesis of these materials.

Keywords: Nanoparticles, microscopy, crystal structure, X-ray absorption spectroscopy.

Introduction

Calcium hydroxide find applications in dentistry [1], bone treatment [2], conservation of cultural heritage [3, 4]. It is also being utilized for desulfurization [5] and CO_2 capture [6]. Alcohol dispersion of this materials is helpful to conserve stone [7]. Thus, attempt were made by researchers to synthesize this material using different approach and different sources. Barbara Salvadori and Luigi Dei synthesize $Ca(OH)_2$ nanoparticles from Diols [8]. Calcium hydroxide nanoparticles of particle size 100 nm and crystallite size ~10.8 nm were synthesized using by hydrogen plasma-Ca reaction method. In this method, Ca ingot covered with oxide layer was used as source [9]. Calcium hydroxide nanoparticles of size ~44 nm was synthesized from calcium nitrate bihydrate and sodium hydroxide [10]. Microwave assisted synthesis of calcium hydroxide from calcium nitrate and sodium hydroxide results in the formation of nanoparticles of size <100 nm [11, 12]. Apart from this, Darroudi *et al*. reported green synthesis of $Ca(OH)_2$ nanoparticles of crystallite size 26 nm from calcium chloride, sodium hydroxide and a biopolymer molecule, gelatin [13]. Thus present work is motivated to synthesize $Ca(OH)_2$ nanoparticles using calcium nitrate.

In recent years, method based on metal nitrates using citric acid as gelatin agent has open ample scope for researchers to synthesize wide variety of materials. This method is successfully utilized for synthesis of different kind of oxides [14-16] and carbonates [17]. This method not only provides better control over stoichiometry but also forms almost spherical particles with relatively narrow size distribution [18, 19].

X-ray diffraction (XRD) is well known tool to investigate the crystal structure of synthesized materials [20, 21]. In addition, this technique also give information about self-induced strain, crystallite size, and microstructural information of synthesized materials [19-21]. Not only, structural behavior but morphological investigation is essential for synthesized material since the shape and size play important roles in determining their efficiency for particular application [1-6]. Scanning electron microscopy has been identified to investigate morphological behavior of nanoparticles. This technique is equally applicable to ceramic system like zirconia [22], titanates [23], and solid-solution [24]. As stated earlier [1-8], $Ca(OH)_2$ is being utilized for several applications which require interaction of continent ions with target material. Hence, there is a need to investigate the behavior of atoms in the lattice and its surroundings. Till date, X-ray absorption spectroscopy is considered to be most sensitive to the valence state and hybridization among different ions [25, 26]. Thus, it not only provides the information of atomic valence state but also reflects its interaction with neighboring atoms [25-28]. Hence, present work is motivated to synthesize calcium hydroxide nanoparticles from calcium nitrate and characterize them for investigation of structural, morphological, and local electronic structure characteristics.

Experimental details

Synthesis

Solution of calcium nitrate tetrahydrate (AR Grade) in stoichiometric proportion were mixed into citric acid

solution by keeping cations to citric acid ratio 1:3 [19]. The mixture was kept on magnetic stirrer at 90°C to get viscous solution for 6 h. The calcium hydroxide nanoparticles (CaH1 and CaH2) were obtained from the subsequently annealing at different temperatures of 800 and 700°C of the dried viscous solution at 100°C for almost 16 h and 40 h, respectively. A schematic of synthesis process is shown in **Fig. 1.**

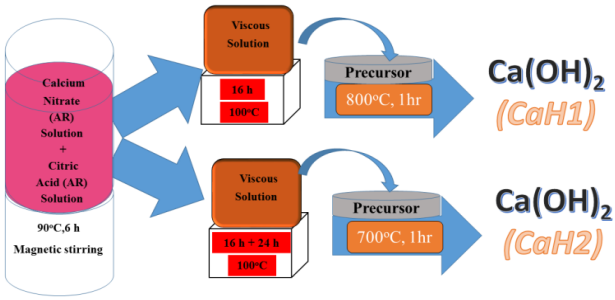

Fig. 1. Schematic utilized for synthesis of calcium hydroxide nanoparticles.

Characterization

XRD patterns of synthesized materials were measured using D/MAX2500(RIGAKU, Japan) X-ray diffractometer at Cu Kα (λ=1.5418 Å) radiation. Scanning electron microscopy (SEM) measurements were performed using Hitachi (S-4200) field emission electron micrographs. Size of various particles was estimated using Image J software. Near edge X-ray absorption fine structure (NEXAFS) measurements on synthesized materials were conducted in ultrahigh vacuum at 10D XAS KIST beamline in Pohang Light Source, Korea. Grating monochromaters with 400 lines/mm and 1000 lines/mm with entrance and exist slits opening of 100μm×100μm were used for recoding Ca *L*- and O *K*-edge NEXAFS spectra for synthesized materials [19]. Ca *K*-edge measurements were performed at 1D XRS KIST-PAL beamline in transmission mode.

Results and discussion

Structural study

Fig. 2 shows XRD patterns of synthesized calcium hydroxide along with XRD pattern of JCPDS No#00-044-1481. These patterns envisage the presence of space group P3m1 in CaH1 and CaH2. It is important to point that phase of $Ca(OH)_2$ is extremely sensitive to the annealing temperature. When both kind of precursors were annealed at different temperatures ranging from 300 to 1200°C, several pure and impure phases appeared. These results are published elsewhere [29, 30]. The crystallite size of these nanoparticles were estimated from Scherrer's formula using most intense peak (101) [11, 14].

$$D = \frac{0.94\lambda}{\beta cos\theta}$$

where, symbols has their usual meanings. The estimated values of crystallite size is shown in **Table 1**. The crystallite size of CaH1 and CaH2 are 10.6±0.7 and 10.8±0.7 nm, respectively for most intense plane (101). Similarly, values of crystallite size estimated from other planes are almost same for CaH1 and CaH2. Thus, crystallite size is not affected by the change of treatment given to precursor along with change in annealing temperature.

Table 1. Crystallite size (D) of synthesized calcium hydroxide estimated from XRD at various planes.

Crystalline Planes	D (nm)	
	CaH1	CaH2
001	14.0±1.8	14.9±1.9
100	15.2±1.2	15.0±1.2
101	10.6±0.7	10.8±0.7
102	7.8±0.4	7.3±0.4
110	15.4±0.6	14.6±0.6
111	11.4±0.4	11.3±0.4

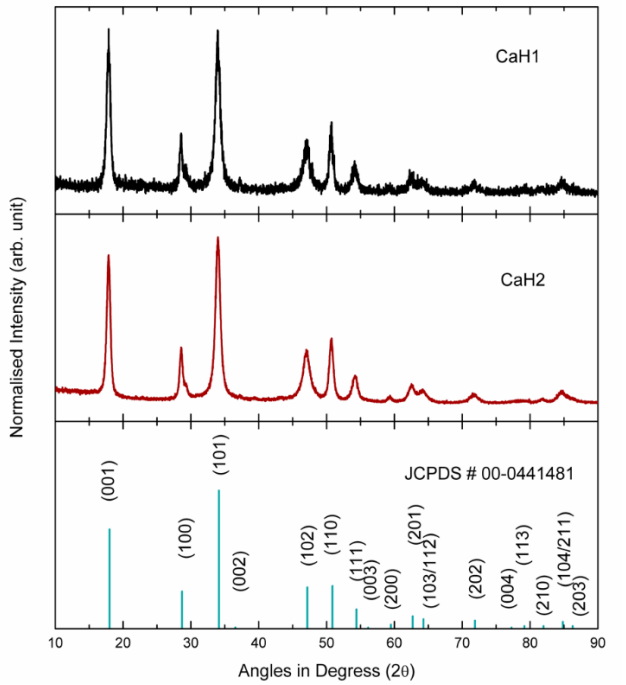

Fig. 2. X-ray diffraction patterns of synthesized $Ca(OH)_2$ nanoparticles.

Morphological study

Fig. 3 and **Fig. 4** shows SEM image of CaH1 and CaH2 at different magnifications. Both systems exhibit bunch of nanoparticles. These nanoparticles seems to be slightly distorted from spherical shape. Particle size distribution diagram of these nanoparticles are shown in **Fig. 5**. The particle size of CaH1 and CaH2 are 55 and 69 nm, respectively. It is observed that nature of distribution is different for both synthesized materials. CaH1 exhibit log-normal distribution of particles, while CaH2 exhibit Gaussian distribution. Thus, the combined annealing sequence can successfully utilized to form tailoring of distribution of particles as well as size of particles without affecting crystallite size.

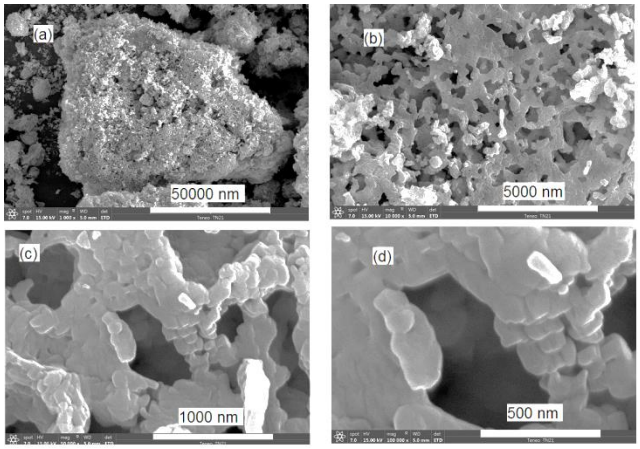

Fig. 3. SEM micrographs of CaH1 at (a) 1k, (b) 10k, (c) 50k, and (d) 100k magnifications.

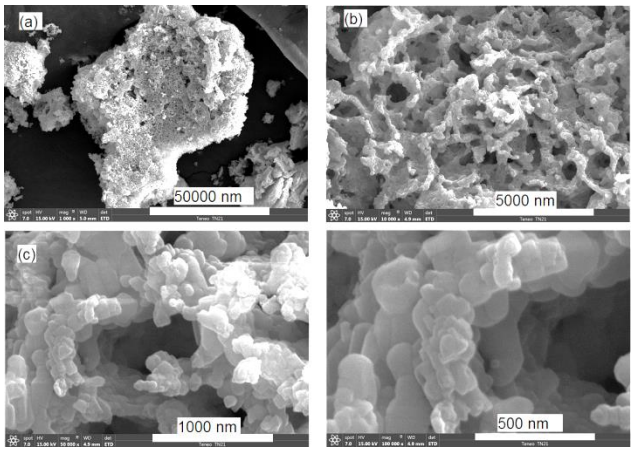

Fig. 4. SEM micrographs of CaH2 at (a) 1k, (b) 10k, (c) 50k, and (d) 100k magnifications.

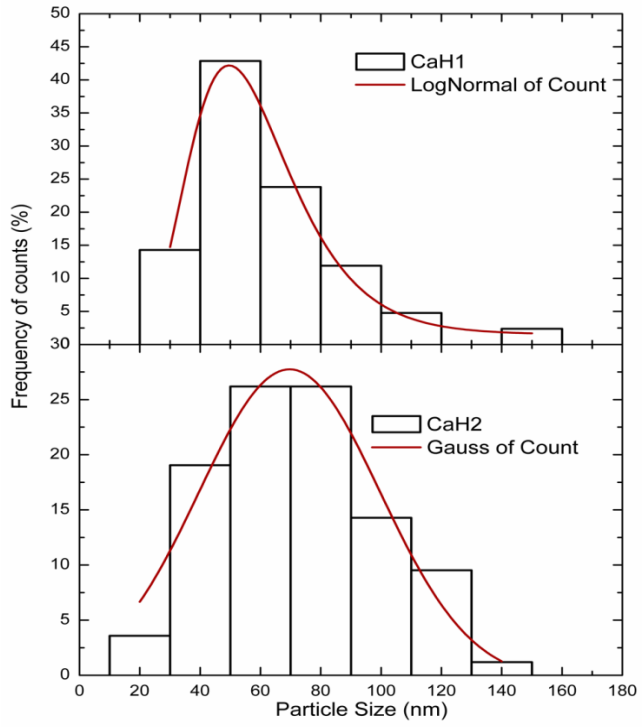

Fig. 5: Particle size distribution of CaH1 and CaH2.

Local Electronic structure study

O K-edge spectra

O *K*-edge NEXAFS spectra of CaH1 and CaH2 exhibit spectral features A_0, A_1, A_2, A_3, A_4, and A_5 are 532.5, 536.0, 539.5, 543.6, 550.5, and 556.5 eV **(Fig. 6)**. These spectral features are well defined and distinguishable in the spectra for both nanoparticle system. The behavior of these spectral features are analogues to that of reported for Portlandite ($Ca(OH)_2$) [28]. The origin of these spectral features is associated with structure of this material. It is well known that $Ca(OH)_2$ is trigonal with the space group P3m1. The structure of this material is regarded as staked sheets of distorted edge sharing Ca-O octahedral along the C-axis [28, 31]. Each –OH group is coordinated by three Ca atoms in its layer and giving rise to sharp spectral features A_1, A_2, and A_3. Presence of sharp spectral features in both CaH1 and CaH2 is associated with $Ca(OH)_2$ phase.

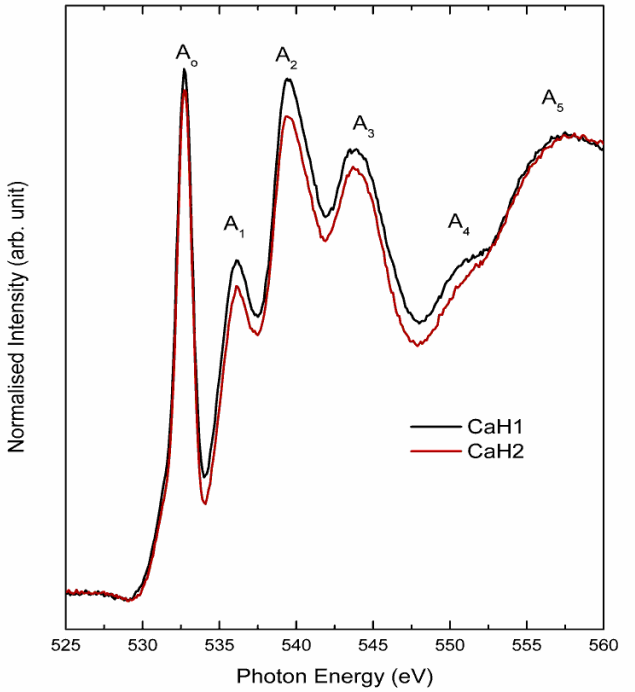

Fig. 6. O *K*-edge NEXAFS spectra of CaH1 and CaH2.

Ca *L*-edge spectra

Ca *L*-edge NEXAFS spectra for CaH1 and CaH2 are shown in **Fig. 7**. These spectra are very much analogues to that of $Ca(OH)_2$ reference reported by Li *et al.* [28]. Spectra for both materials exhibit spectral features B_1, B_2, B_3, and B_4 centered at 347.8, 349.2, 351.2, and 352.5 eV **(Table 2)** followed by a pre-peak structure shown by shaded region in **Fig 7**. This pre-edge structure also observed in number of Ca compounds reported by Naftel *et al*., however no explanation is provided [32]. Spectral features B_1 and B_2 are associated with spin-orbit related peak L_3 and B_3 and B_4 to that of L_2. Observed splitting among L_3 and L_2 is known to be the crystal field arising from the symmetry of atoms surrounding the Ca^{2+} ion in

the first co-ordination sphere. Thus assigned to t_{2g} and e_g symmetry states [17, 29, 33]. The splitting of t_{2g} and e_g is generally related with crystal field parameter [34]. In present case, this splitting is 1.2±0.2 eV for both systems **(Table 2)** and is equivalent to the value reported for similar systems [32]. The value of t_{2g}/e_g ratio is close to 0.4 for L_3 and L_2 related peaks for CaH1 and CaH2 **(Table 2).** Thus, these values signify that strength and magnitude of crystal field parameters remain same in CaH1 and CaH2. This value does not affected change of thermal treatment during the process of synthesis.

Table 2. Energy difference and intensity ratio of t_{2g} and e_g features of Ca *L*-edge NEXAFS spectra for CaH1 and CaH2.

Spectral features	Position (eV)	Intensity	Energy difference (t_{2g} ~ e_g)	Intensity ratio (t_{2g}/e_g)
CaH1				
Pre-peak	346.9±0.1	0.13±0.05		
B_1	347.9±0.1	0.80±0.05	1.2±0.2	0.36
B_2	349.1±0.1	2.19±0.05		
B_3	351.2±0.1	1.09±0.02	1.2±0.2	0.40
B_4	352.4±0.1	2.69±0.05		
CaH2				
Pre-peak	346.9±0.1	0.06±0.04		
B_1	347.9±0.1	0.70±0.05	1.2±0.2	0.41
B_2	349.1±0.1	1.70±0.05		
B_3	351.2±0.1	0.83±0.02	1.2±0.2	0.39
B_4	352.5±0.1	2.11±0.05		

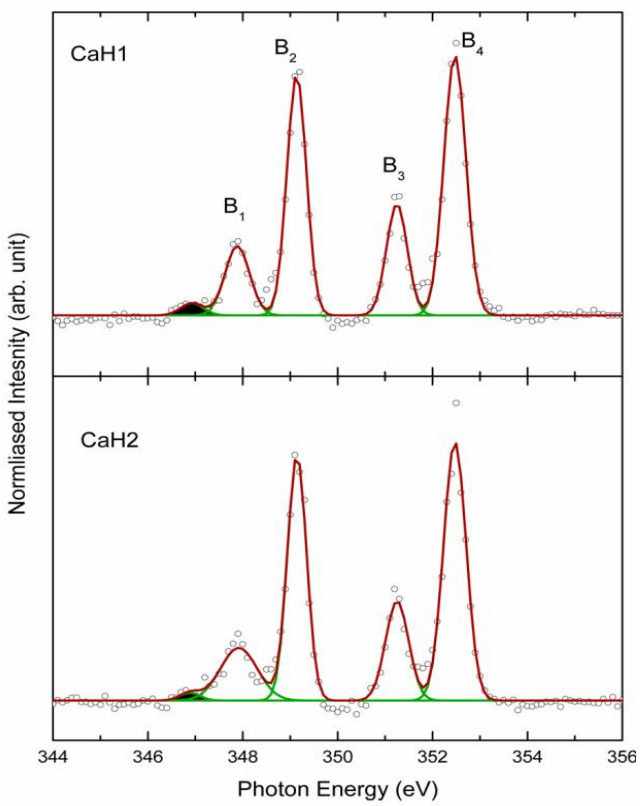

Fig. 7. Ca *L*-edge NEXAFS spectra of CaH1 and CaH2.

Ca K-edge spectra

In **Fig. 8,** Ca *K*-edge spectra of CaH1 and CaH2 are shown. The shape of these spectra resemble with the spectra reported for calcium hydroxide [35, 36]. Both spectra consists of pre-edge structure around 4040 eV (C_1) and a shoulder like structure at 4045 eV (C_2) along with two main peaks centered at 4048 (C_3) and 4049 eV (C_4). Pre-edge structure is assigned to originate from 1*s* to bound 3*d* orbitals, while the presence of shoulder is attributed to that of 1*s* to 4*s* transitions (quadrupole) [27, 38]. Spectral features C_3 and C_4 occurs due to 1*s* to $4p_{1/2}$, as well as 1**s** to $4p_{3/2}$ (dipole-) transitions, respectively [37]. Splitting among C_3 and C_4 is dominant compared to other Ca based compounds [35-37]. Thus both materials exhibit Ca *K*-edge spectra, typical of $Ca(OH)_2$.

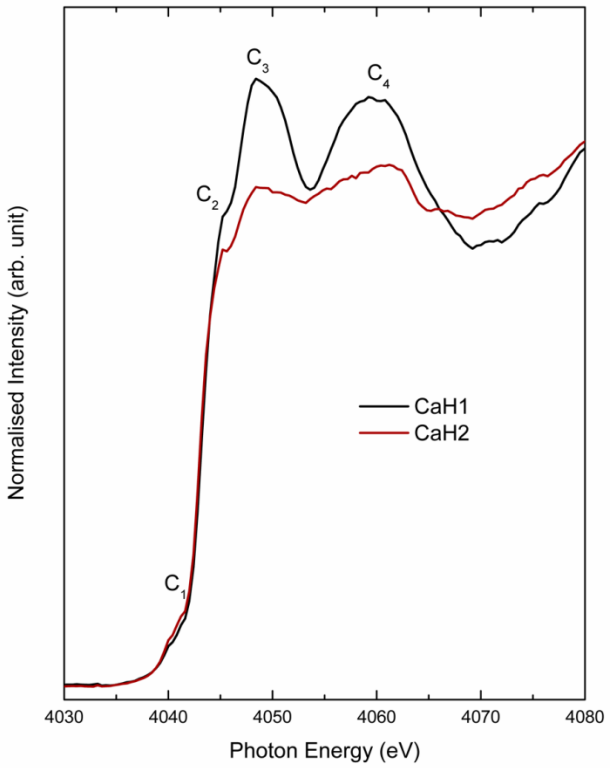

Fig. 8. Ca *K*-edge NEXAFS spectra of CaH1 and CaH2.

Conclusion

Thus, we have successfully synthesized calcium hydroxide nanoparticle from modified sol-gel method. These nanoparticles exhibit trigonal structure with space group P3m1 space group. Though average crystallite size is not affected by synthesizing procedure but it affects the particle size of these nanoparticles. Moreover, the size distribution of these nanoparticles are affected by the thermal treatment. Local electronic structure of these materials remain unaffected with thermal treatment.

Acknowledgment

This work is supported by Korea Institute of Science and Technology, Seoul, Korea (KIST Project No. 2V04611).

References

1. Khaled A Balto, Calcium hydroxide has limited effectiveness in eliminating bacteria from human root canal, British Dental Journal 218 (2015) 19.
2. J. Heer, Calcium hydroxide therapy and bony regeneration following autogenous tooth transplantation: case report and three year follow up, British Dental Journal 203 (2007) 403 – 405.
3. G. Poggi, N. Toccafondi, L. N. Melita, J. C. Knowles, L. Bozec, R. Giorgi, P. Baglioni, Calcium hydroxide nanoparticles for the conservation of cultural heritage: new formulations for the deacidification of cellulose-based artifacts, Applied Physics A 114 (2014) 685–693.
4. Carlos Rodriguez-Navarro, Irene Vettori, and Encarnacion Ruiz-Agudo, Kinetics and Mechanism of Calcium Hydroxide Conversion into Calcium Alkoxides: Implications in Heritage Conservation Using Nanolimes, Langmuir, 32 (2016) 5183–5194.
5. Sheng Chu, Cheng Zhu, Geoffrey A. Tompsett, T. J. Mountziaris, and Paul J. Dauenhauer, Refuse-Derived Fuel and Integrated Calcium Hydroxide Sorbent for Coal Combustion Desulfurization, Ind. Eng. Chem. Res., 54 (2015) 3136–3144.
6. Sang-Jun Han, Miran Yoo, Dong-Woo Kim, and Jung-Ho Wee, Carbon Dioxide Capture Using Calcium Hydroxide Aqueous Solution as the Absorbent, Energy Fuels, 25 (2011) 3825–3834.
7. Carlos Rodriguez-Navarro, Amelia Suzuki, and Encarnacion Ruiz-Agudo, Alcohol Dispersions of Calcium Hydroxide Nanoparticles for Stone Conservation, Langmuir, 29 (2013) 11457–11470.
8. Barbara Salvadori and Luigi Dei, Synthesis of $Ca(OH)_2$ Nanoparticles from Diols, Langmuir, 17 (2001) 2371–2374.
9. Tong Liu, Yarong Zhu, Xuanzhou Zhang, Tongwen Zhang, Tao Zhang, Xingguo Li, Synthesis and characterization of calcium hydroxide nanoparticles by hydrogen plasma-metal reaction method, Materials Letters, 64 (2010) 2575–2577.
10. Aniruddha Samanta, Dipak K. Chanda, Pradip Sekhar Das, Jiten Ghosh, Anoop Kumar Mukhopadhyay, Arjun Dey, Synthesis of Nano Calcium Hydroxide in Aqueous Medium, J. Am. Ceram. Soc., 99 (2016) 787–795.
11. Khaled M. Saoud, Imen Ibala, Dana El Ladki, Omar Ezzeldeen, and Shaukat Saeed, Microwave Assisted Preparation of Calcium Hydroxide and Barium Hydroxide Nanoparticles and Their Application for Conservation of Cultural Heritage, Digital Heritage. Progress in Cultural Heritage: Documentation, Preservation, and Protection, Lecture Notes in Computer Science 8740 (2014) 342-352.
12. G. Taglieri , C. Mondelli , V. Daniele , E. Pusceddu , A. Trapananti, Synthesis and X-Ray Diffraction Analyses of Calcium Hydroxide Nanoparticles in Aqueous Suspension, Advances in Materials Physics and Chemistry, 3 (2013) 108-111.
13. Majid Darroudi, Maryam Bagherpour, Hasan Ali Hosseini, Mahmoud Ebrahimi, Biopolymer-assisted green synthesis and characterization of calcium hydroxide nanoparticles, Ceramics International, 42 (2016) 3816–3819.
14. Parmod Kumar, Jitendra Pal Singh, Yogesh Kumar, Anurag Gaur, Hitendra K. Malik, K. Asokan, Investigation of phase segregation in $Zn_{1-x}Mg_xO$ systems, Current Applied Physics, 12 (2012) 1166–1172.
15. Jitendra Pal Singh, RC Srivastava, HM Agrawal, RPS Kushwaha, Prem Chand, Ravi Kumar, EPR study of nanostructured zinc ferrite, International Journal of Nanoscience, 7 (2008) 21-27.
16. A. E. Danks, S. R. Hall and Z. Schnepp, The evolution of 'sol–gel' chemistry as a technique for materials synthesis, Mater. Horiz., 3 (2016) 91-112.
17. Jitendra Pal Singh, Weon Cheol Lim, Sang Ok Kim, Keun Hwa Chae, Synthesis and Local Electronic Structure of Calcite Nanoparticles, Journal of Nanoscience and Nanotechnology (in Press).
18. Jitendra Pal Singh, Gagan Dixit, Hemaunt Kumar, R.C. Srivastava, H.M. Agrawal, Ravi Kumar, Formation of latent tracks and their effects on the magnetic properties of nanosized zinc ferrite, Journal of Magnetism and Magnetic Materials, 352 (2014) 36–44.
19. Jitendra Pal Singh, So Hee Kim, Sung Ok Won, Weon Cheol Lim, Ik-Jae Lee, Keun Hwa Chae, Covalency, hybridization and valence state effects in nano-and micro-sized $ZnFe_2O_4$, CrystEngComm, 18 (2016) 2701-2711.
20. Alberto Viani, Konstantinos Sotiriadis, Adél Len, Petr Šašek, Radek Ševčík, Assessment of firing conditions in old fired-clay bricks: The contribution of X-ray powder diffraction with the Rietveld method and small angle neutron scattering, Materials Characterization, 116 (2016) 33-43
21. Tibor Berecz, Péter Jenei, András Csóré, János Lábár, Jenő Gubicza, Péter János SzabóDetermination of dislocation density by electron backscatter diffraction and X-ray line profile analysis in ferrous lath martensite, Materials Characterization, 113 (2016) 117-124
22. Mahmood Sheikhattar, Hooyar Attar, Shahriar Sharafi, William M. Carty, Influence of surface crystallinity on the surface roughness of different ceramic glazes, Materials Characterization, 118, (2016) 570–574
23. Pei Chen, Yantao Zhang, Fengqi Zhao, Hongxu Gao, Xinbing Chen, Zhongwei An, Facile microwave synthesis and photocatalytic activity of monodispersed $BaTiO_3$ nanocuboids, Materials Characterization, 114 (2016) 243–253
24. Ruoshan Lei, Mingpu Wang, Huanping Wang, Shiqing Xu, New insights on the formation of supersaturated Cu-Nb solid solution prepared by mechanical alloying, Materials Characterization 118 (2016) 324–331
25. Claudia S. Schnohr and Mark C. Ridgway, Introduction to X-Ray Absorption Spectroscopy, © Springer-Verlag Berlin Heidelberg 2015 C.S. Schnohr and M.C. Ridgway (eds.), X-Ray Absorption Spectroscopy of Semiconductors, Springer Series in Optical Sciences 190, **DOI:** 10.1007/978-3-662-44362-0_1.
26. Junko Yano, Vittal K. Yachandra, X-ray absorption spectroscopy, Photosynth Res 102 (2009) 241–254.
27. Tae-Hyun Kim, Il Heo, Seung-Min Paek, Chung-Berm Park, Ae-Jin Choi, Sung-Han Lee, Jin-Ho Choy,and Jae-Min Oh, Layered Metal Hydroxides Containing Calcium and Their Structural Analysis, Bull. Korean Chem. Soc. 33 (2012) 1845-1850.
28. Qinfei Li, Yong Ge, Guoqing Geng, Sungchul Bae, and Paulo J. M. Monteiro, CaCl2-Accelerated Hydration of Tricalcium Silicate: A STXM Study Combined with ^{29}Si MAS NMR, Journal of Nanomaterials, 2015 (2015) 215371.
29. Jitendra Pal Singh, Weon Cheol Lim, Sung Ok Won and K. H. Chae, Effect of precursor history on the formation of amorphous and crystalline calcium carbon'ate, Particulogy .
30. Jitendra Pal Singh, Sung Ok Won and Keun Hwa: On the synthesis of selected alkaline oxides using magnesium nitrate in citric acid matrix (To be communicated).
31. T. Nagai, T. Ito, T. Hattori, and T. Yamanaka, Compression mechanism and amorphization of portlandite, $Ca(OH)_2$: structural refinement under pressure, Physics and Chemistry of Minerals, 27 (2000) 462–466.
32. S.J. Naftela T.K. Sham,a Y.M. Yiua , and B.W. Yates, Calcium L-edge XANES study of some calcium compounds, J. Synchrotron Rad. 8 (2001) 255-257.
33. Y. U. T. Gong, C. E. Killiana, I. C. Olson, N. P. Appathurai, A. L. Amasino, M. C. Martin, L. J. Holt, F. H. Wilt, and P. U. P. A. Gilbert, PNAS, 109 (2012) 6088.
34. F. M. F. de Groot, J. C. Fuggle, B. T. Thole, and G. A. Sawatzky, Phys. Rev. B 41 (1990), 928-937.
35. Jie Hu, Lijuan Liu, Mingqi Cui, Jie Wang, Calcium-promoted catalytic activity of potassium carbonate for gasification of coal char: The synergistic effect unrelated to mineral matter in coal, Fuel 111 (2013) 628–635.
36. Liu Li-Juan, Liu Hui-Jun, Cui Ming-Qi, Hu Yong-Feng, Zheng Lei, Zhao Yi-Dong, Ma Chen-Yan, Xi Shi-Bo, Yang Dong-Liang, Guo Zhi-Ying, Wang Jie, Determination of the calcium species in coal chars by Ca K-edge XANES analysis, Chinese Physics C 37 (2013) 028003.
37. Bernhard Hesse, Murielle Salome, Hiram Castillo-Michel, Marine Cotte, Barbara Fayard, Christoph J. Sahle, Wout De Nolf, Jana Hradilova, Admir Masic, Birgit Kanngießer, Marc Bohner, Peter Varga, Kay Raum, and Susanne Schrof, Full-Field Calcium K-Edge X-ray Absorption Near-Edge Structure Spectroscopy on Cortical Bone at the Micron-Scale: Polarization Effects Reveal Mineral Orientation, Anal. Chem. 88 (2016) 3826-3835.

